Nanocapsules

DOI: 10.1002/ange.201405148

Chemical Sealing of Nanotubes: A Case Study on Sb_2S_3**

*Suresh Sarkar, Amit K. Guria, Biplab K. Patra, and Narayan Pradhan**

Abstract: *Implementing the solution chemistry, herein, we report the sealing of both ends of Sb_2S_3 semiconductor nanotubes following the diffusion-controlled deposition of the sealing material, $AgSbS_2$. As a consequence, unique dumbbell-shaped hollow nanocapsules having a binary–ternary epitaxial heterojunction were formed in solution. Whereas these capsule-shaped nanostructures were obtained by the introduction of Ag^0 nanocrystals just after the formation of Sb_2S_3 nanotubes, the addition of Ag^0 at the beginning of the process, prior to the formation of nanotubes, changed the growth pattern, and solid nanorods of Sb_2S_3 were formed. The details of the chemistry involved in the formation of these nanostructures were investigated and are discussed herein.*

Nanotubes are one of the special kind of nanomaterials whose architecture needs a different growth pattern than that of the solid 1D nanostructure.[1] These nanomaterials have structure-dependent properties with wide application in electron transport, devices, sensors, storage materials, and catalysis.[2] There has been a revolution in the architecture of different nanomaterials, and several fascinating nanostructures have been developed,[3] but little attention has been paid to these hollow tubular-shaped nanostructures. When the architectural parameters are controlled, nanotubes can also be functional materials like other well-studied 0D, 1D, and 2D solid nanostructures. Furthermore, the hollow nanostructure can also be transformed into capsule-shaped or hybrid hollow nanostructures by the sealing of their exposed ends with the same or a different material. The difficulty in designing such hybrid functional nanomaterials is related to the complicated formation mechanism of nanotubes, which normally proceeds through template synthesis or sheet wrapping mechanism.[1,4] Moreover, to date, the sealing or closing of nanotubes with the same materials remains unrealistic, as it requires a different growth pattern at the exposed ends to that for tube formation. Furthermore, epitaxy formation is essential for either sealing or creation of heterojunction at the edge of the exposed ends of the tubes,and this process also depends on the availability of energetically favorable facets in the materials. Hence, the sealing of nanotubes needs a special strategy, and even after decades, when nanomaterials synthesis seems to have been covered quite comprehensively, research in this direction has yet to be explored.

Previous studies have revealed that the key factor in tuning the shape of the nanostructures is solution chemistry, which regulates the surface–ligand binding, interface chemistry, and the creation of facets of different reactivity.[5] Recently, it was shown that apart from solution chemistry, simply the introduction of some selective ionic impurities can alter the route of an ongoing growth process and drastically affect the shape and phase of the host nanostructures.[5c,d,6] These results suggest that several possibilities for the design and synthesis of such nanostructures remain to be discovered. Moreover, all these exciting studies in solution chemistry have dealt with solid nanostructures rather than the tubular or hollow 1D nanostructures.

We report herein the formation of high-quality tubular nanostructures of Sb_2S_3, as a model semiconductor system, by the thermal decomposition of a single-source precursor in solution. We studied the effects of Ag^0 by introducing it at different stages of the reaction. We observed that the treatment of Ag^0 particles just after the formation of the nanotubes sealed both ends of the tube during annealing and led to dumbbell-shaped hollow nanocapsules with a binary–ternary semiconductor heterojunction. Interestingly, when Ag^0 was introduced at the beginning of the reaction, prior to nanotube formation, it altered the reaction process and resulted in the formation of 1D solid nanorods of Sb_2S_3 instead of dumbbell-shaped hollow nanostructures. In one case, the Ag^0 formed $AgSbS_2$ ternary semiconductors at the exposed ends of Sb_2S_3 tubes with clear phase separation by a diffusion mechanism to seal the tubes; in the other case, it was doped into the lattice of the Sb_2S_3 nanorod. We report herein architectures beyond the nanotube and discuss the chemistry used for the formation of nanocapsules of inorganic materials by colloidal techniques. Furthermore, the mechanistic aspects of the formation of the 1D heterostructures with an internal hollow space and the effect of the mode of introduction of foreign ions were investigated and are discussed herein.

Antimony sulfide is known for the formation of tubular nanostructures.[1c,7] The synthesis of hollow tubes of Sb_2S_3 by a solvothermal method[4a] and a chemical-vapor-transport method[7b] has been reported previously. Herein, we describe the synthesis of high-quality hollow nanotubes on the basis of a colloidal technique by the thermal decomposition of the single-source precursor antimony diethyldithiocarbamate (Sb-DDTC) in a coordinating alkyl amine solvent at about 210–220 °C. The alkyl thiol *tert*-dodecylmercaptan (2,3,3,4,4,5-hexamethyl-2-hexanethiol) was introduced as a growth-controlling agent and to maintain good dispersion of the nanotubes. The introduction of silver at different stages of the reaction led to different nanostructures. The evolution of

[*] S. Sarkar, A. K. Guria, B. K. Patra, Dr. N. Pradhan
Department of Materials Science and Centre for Advanced Materials
Indian Association for the Cultivation of Science
Kolkata 700032 (India)
E-mail: camnp@iacs.res.in
Homepage: http://iacs.res.in/matsc/msnp/

[**] The DST of India (SR/ST/IC-68/2010, SJF/CSA-01/2010-11) is acknowledged for funding.

Supporting information for this article is available on the WWW under http://dx.doi.org/10.1002/anie.201405148.

different nanostructures with and without Ag^0, and according to the timing of its introduction, is illustrated in Figure 1.

Figure 2 a,b shows high-angle annular dark field (HAADF) and transmission electron microscopy (TEM) images (see also Figure S1 in the Supporting Information) of the nanotubes formed, which had a diameter of approximately 120–150 nm and a length of approximately 1200–1500 nm. A high-resolution TEM (HRTEM) image (Figure 2 c) suggests that the phase of the nanostructure is orthorhombic and the tube is viewed along the [101] direction. The observed planes showed *d* spacings of 0.79 and 0.345 nm corresponding to the (101) and (11-1) planes of bulk orthorhombic Sb_2S_3, respectively. An atomic model corresponding to the HRTEM image with a similar viewing direction is depicted in Figure 2 d. The peak positions in an X-ray powder diffraction pattern of the nanotubes (Figure 3) correspond to the orthorhombic phase of Sb_2S_3 (JCPDF #741046).

These nanotubes were typically formed at 210 °C with an annealing time of 15 min, which allowed almost complete decomposition of the single-source precursor, and became crystalline during the course of annealing. For the synthesis, a suspension of Sb-DDTC in a mixture of oleylamine and *tert*-dodecylmercaptan was swiftly injected into hot 1-hexadecyl-

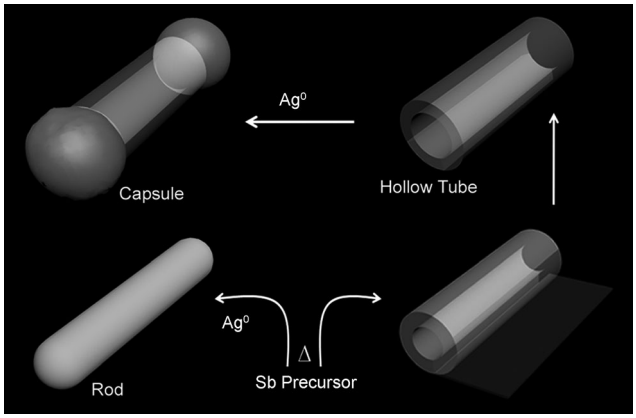

Figure 1. Sb_2S_3 tube formation and the evolution of different kinds of nanostructures depending on the timing of the introduction of Ag^0. Whereas the introduction of Ag^0 prior to tube formation results in solid nanorods, post treatment of Ag^0 into the nanotubes produces phase-separated ternary $AgSbS_2$ at the exposed ends of the tubes to form capsule-shaped nanostructures.

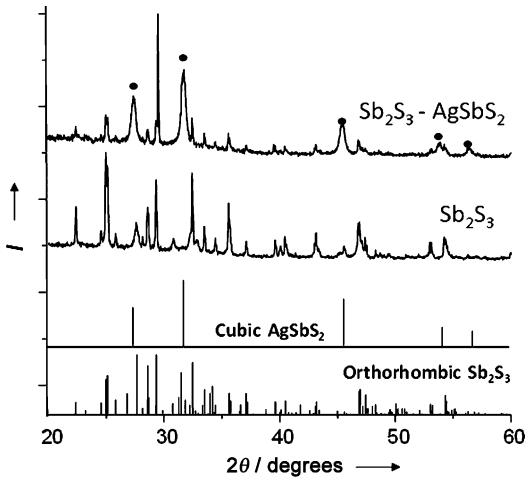

Figure 3. Powder XRD patterns of Sb_2S_3 nanotubes and Sb_2S_3–$AgSbS_2$ sealed nanotubes. Peaks marked with dots are not observed for Sb_2S_3 and are thus assigned to cubic $AgSbS_2$.

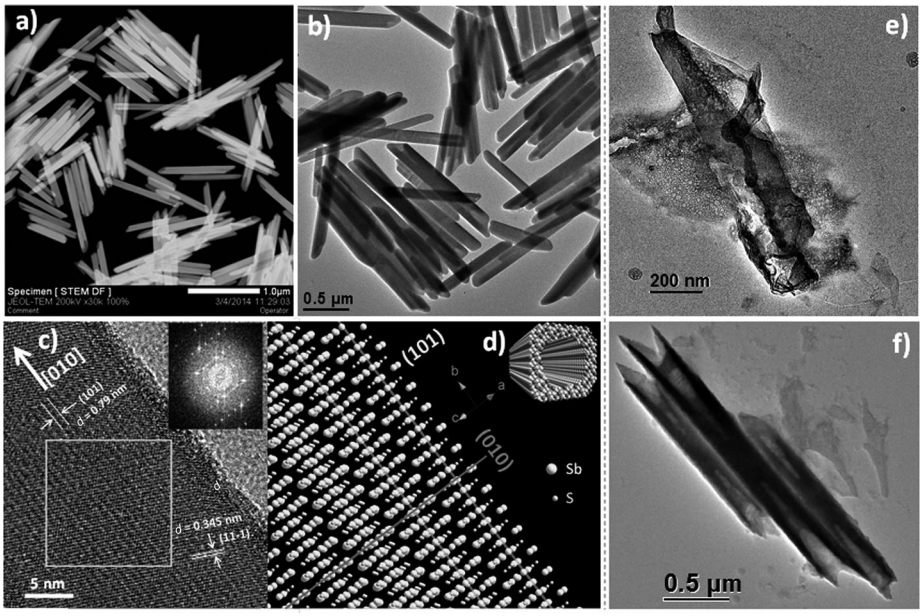

Figure 2. a) HAADF-STEM and b) bright-field TEM images of Sb_2S_3 nanotubes. c) HRTEM image of a Sb_2S_3 nanotube and d) an atomic model constructed on the basis of the HRTEM image. The inset in (c) is the selected-area FFT pattern, and that in (d) shows an atomic model of the tube viewed along the major axis. e,f) TEM images of the intermediate samples showing tube formation through the rolling of sheets.

amine in the reaction flask. Tube formation was readily detected by the naked eye, as the solution color changed from orange to black soon after the injection of the precursors (within 5 min). To understand the formation mechanism, we collected the intermediate samples at different stages of the reaction. Interestingly, we observed that these tubes are formed through the rolling of thin sheets (Figure 2 e,f; see also Figure S2). A similar mechanism was predicted previously for a larger Sb_2S_3 tube synthesized by the chemical-vapor-transport method.[7b] However, in this study, we captured the intermediate with proper control of formation by a colloidal technique.

Herein, we mostly focus on architecture beyond nanotubes for the design of new functional

materials through the sealing of two open ends of the tube with different semiconductor materials. It has been established that with Sb^{3+}, Ag^{+} can form ternary sulfide compounds.[8] Considering this advantage, we introduced AgCl dissolved in oleylamine at 220 °C into the reaction system after the formation of the nanotubes. It is known that AgCl forms Ag^0 when heated in a fatty amine,[9] as reflected by the plasmon absorption of the solution (see Figure S3). Upon the introduction of these preformed Ag^0 particles into the reaction flask containing Sb_2S_3 nanotubes just after their formation, the new semiconductor material was found to deposit on both open ends of the tubes. Furthermore, by examining the reaction mixture at different stages of the reaction, we observed that the two open ends of the tubes were entirely sealed during the course of annealing. The disappearance of Ag^0 particles was reflected by the prompt diminishment of the corresponding plasmon absorption. Typical TEM and HAADF images of the (nanocapsule-like) dumbbell-shaped hollow sealed tubes are shown in Figure 4 (see Figures S4 and S5 for more images). The contrast differences in both bright- and dark-field images (Figure 4a–e) between the tips and the tubes clearly suggest the existence of two distinct shapes and phase boundaries in this hybrid nanostructure. Elemental mapping (Figure 4b, right) suggests that the tips of this nanocapsule contain Ag, Sb, and S, whereas the tube portion contains only Sb and S. Energy-dispersive X-ray spectroscopy (EDX) of the tip area confirms the presence of nearly equal atomic percentages of Ag and Sb (see Figure S6), thus indicating that the material might be $AgSbS_2$. This composition was confirmed by the measurement of more than five different tips of this hybrid nanostructure. The skeleton of the nanostructure remained hollow, as reflected by the intensity profile of the line scan elemental mapping data (see Figure S7). By subtracting the peaks of Sb_2S_3 hollow tubes from the XRD patterns of these hollow dumbbells (Figure 3), it was confirmed that $AgSbS_2$ was in the cubic phase (JCPDF #170456). Accordingly, we analyzed the HRTEM image and studied epitaxy formation at the interface. The TEM images in Figure 4 f,g show a clear junction between the two semiconductors. Simulated HRTEM images of the marked areas (1 and 2) in Figure 4 f show the different planes with their *d* spacings. Corresponding atomic models are also depicted on the right. Details of the fast Fourier transforms (FFTs) of the selected areas 1 and 2 are shown in Figure S8 of the Supporting Information. From the analysis, it was observed that the (012) plane of the binary Sb_2S_3 nanotubes closely matches the (111) plane distance of ternary $AgSbS_2$. In the two phases, the *b* axis remains parallel, which suggests that the epitaxy is formed along the [010] direction of both materials.

The major issues that remain here are how the sealing occurs and what the driving forces are for the creation of the phase-separated ternary materials at both ends of the tubes. We first analyzed the hurdles and the practical difficulties in designing such sealed hollow tubular nanostructures. It is clear that the procedure for the formation of these nanostructures is different to that for solid rods, as the nanostructures are cylindrical in shape with a hollow space inside. To seal these tubes, a different kind of growth pattern is required at the exposed end of the tube. Typically, it is difficult for the same constituent to seal the open ends of the tube, as tube formation follows the conventional mechanism of sheet wrapping. Hence, possibly, it would be easier for a different material to nucleate at the exposed ends of the tube, and this material would grow differently and seal the open ends of the tubes during the subsequent stages of the reaction. Furthermore, if a preformed particle of the same or a different material occupies the exposed ends of the tube, it might entirely block the open ends of the tube through epitaxy formation at the interface. Neither of these strategies seems straightfor-

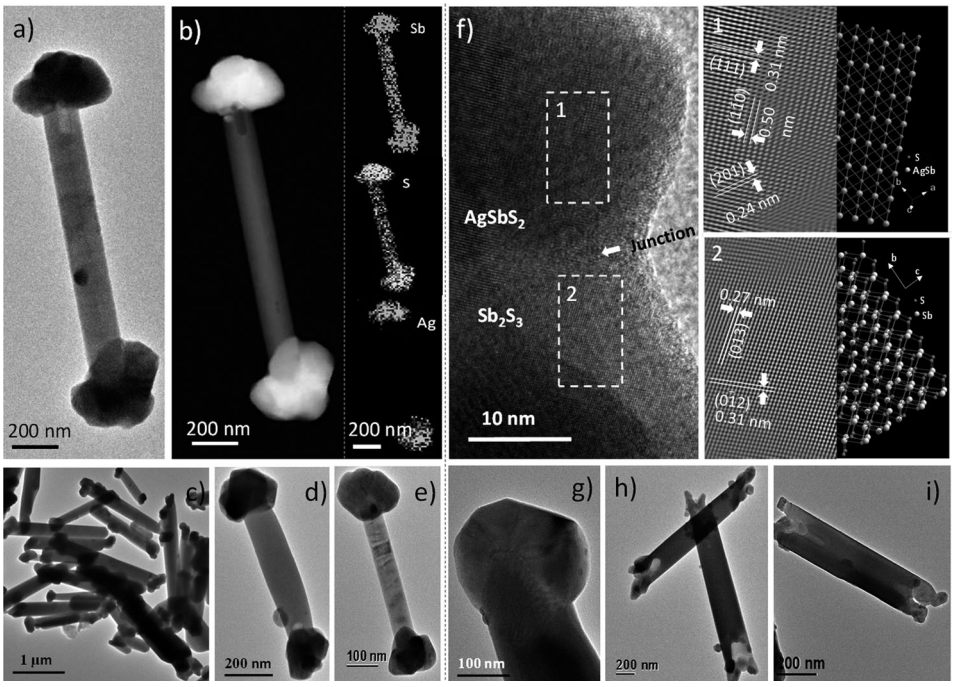

Figure 4. a) TEM and b) HAADF-STEM image of a typical sealed nanotube. The right-hand image in (b) shows the mapping of elements Sb, S, and Ag. c) Wide view of a TEM image showing sealed tubes. d,e) TEM images of single sealed tubes. f) HRTEM image showing the heterojunction. The simulated HRTEM images and representative atomic models from the selected areas 1 and 2, which present $AgSbS_2$ and Sb_2S_3, respectively, are also shown next to the corresponding HRTEM images. The viewing direction for $AgSbS_2$ and Sb_2S_3 is [112] and [100], respectively. g) Magnified TEM image showing the junction of the two materials. h,i) Intermediate TEM images showing patches of the $AgSbS_2$ material at both ends of the tubes.

ward for a colloidal method, as such procedures need sophisticated reaction techniques and extreme control over the reaction path. The most important factor is the lattice matching of the appropriate facets of the sealing materials with the exposed facets at the two ends of the tube. Hence, the selection of the sealing material remains the key issue for the synthesis of the capsule-shaped nanostructure from a nanotube. Previous studies have revealed that dumbbell-shaped nanostructures with noble-metal tips typically have solid 1D nanostructures.[10] In these cases, the rods provide a greater interfacial area, whereby lattice continuity and epitaxy formation with the 0D particles are relatively straightforward. In contrast, such epitaxy formation with exposed ends of the nanotube is difficult from a practical point of view. We therefore sought to uncover the mechanism of this unusual chemical-sealing protocol based on a colloidal technique.

To investigate this mechanism, we recorded images of nanostructures at an intermediate stage of the reaction (Figure 4h,i). These images suggest that small patches of new materials are deposited randomly on the open ends of the tubes. Further analysis of several more TEM images (see Figure S9) led us to conclude that the deposition of these materials in patches continues until the open ends are entirely blocked. As the control reaction without Ag^0 produced only hollow nanotubes, it can be assumed that Ag^0 initiates the formation of the new material at the exposed ends of Sb_2S_3 tubes. We observed neither pure Ag^0 particles nor silver sulfide directly attached to the tubes. The peaks in an XRD spectrum of the sample collected a few minutes after the injection of Ag^0 nanocrystals (within 10 min) resembled those of the final product. Hence, we predict that the Ag^0 particles while dispersed in the reaction medium target the open ends of the tube, and then the diffusion of Sb and S into Ag^0 or vice versa initiates the formation of $AgSbS_2$ (see Figure S10 for a schematic representation of the sealing of a tube by ternary materials). A similar diffusion mechanism was also reported for different silver- or copper-based ternary semiconductor nanocrystals.[11] However, in this study it was explored for the first time with respect to Sb_2S_3 tubular nanostructures. Furthermore, we suggest that the Ag^0 particles target simultaneously both exposed ends of the tube, which are less passivated and therefore more reactive than the main part of the tube, to initiate the formation of $AgSbS_2$, which has a different growth pattern to that of the nanotube. As discussed above, the tubes are formed by a sheet-wrapping mechanism and do not have alternate cation and anion facets along the major axis as typically observed in the 1D nanostructure (in the wurtzite phase).[3a] Moreover, both Sb and S atoms are present in both exposed (101) facets, and consequently, the alternative adsorption of cations and anions is less probable in this case. Hence, the diffusion of Sb^{3+} and S^{2-} to Ag^0 or vice versa is the expected mechanism for the formation of the new material that seals both exposed ends of the nanotubes. The epitaxy formation also relates to the minimum lattice mismatch between Sb_2S_3 and $AgSbS_2$ along the favorable direction [010]. Hence, the entire sealing process follows the strategy based on the control of solution chemistry for the formation of binary and ternary semiconductor junction.

While investigating the timing of Ag^0 introduction into the reaction medium, we observed that the entire procedure of sheet wrapping and the formation of hollow binary Sb_2S_3 tubes can take a different turn. When the Ag^0 particles at a much lower concentration ($<10\%$ relative to Sb) are introduced at the beginning of the reaction, prior to the formation of the tubes, solid nanorods rather the hollow nanostructures are formed. Figure 5a shows a representative

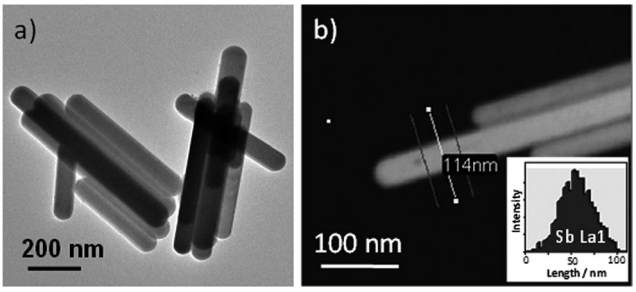

Figure 5. a) TEM image of the nanorods. b) HAADF image and line scan for the element Sb in a typical rod. The inset in (b) shows the counts of Sb with respect to length for a single nanorod.

TEM image of Sb_2S_3 nanorods obtained by introducing Ag^0 particles before the injection of Sb-DDTC into the hot alkyl amine solvent. These nanostructures are solid 1D structures, as supported by line scan elemental mapping, in which the counts of the elements varied with the thickness of the nanostructures (Figure 5b). The rods possessed the same orthorhombic phase (see XRD pattern in Figure S11a) as observed for the hollow Sb_2S_3 nanotubes. Elemental analysis (EDX) suggests that these nanostructures contain approximately 1% Ag (relative to Sb; see Figure S12). To understand the mechanism, we trapped intermediate samples (see Figure S13), and observed that the nanorods are also formed from Sb_2S_3 sheets. In this case, the added Ag^0 particles are expected to be converted into silver antimony sulfide (see XRD pattern in Figure S11b) and are attached to the sheets, which hinders the rolling of sheets as required for tube formation and rather facilitates rod formation through squeezing of the sheets. Initially, the rods were found to be formed with uneven diameters (see Figure S13), and during the course of annealing the diameters become uniform. This proposed mechanism is in contrast to the formation of typical 1D nanostructures, whereby cations and anions are alternatively adsorbed on the reactive polar facets of the nanostructures. However, the core mechanism for the formation of these solid nanorods requires further investigation. Undoubtedly, both the rods and the tubes are formed from the thin sheets by different growth processes.

In conclusion, we have reported herein the chemical sealing of hollow nanotubes in solution. By the simple addition of Ag^0 impurity, the hollow nanotubes of Sb_2S_3 were successfully sealed, and the internal hollow space was maintained. Functionally, this strategy led to a new material, Sb_2S_3–$AgSbS_2$, with a binary–ternary semiconductor heterojunction. Tube formation and sealing did not occur, but

instead solid 1D nanorods were formed, when the Ag^0 impurity was introduced prior to nanotube formation. Our results suggest that although an enormous amount of research has been carried out in the development of new protocols for the designing of colloidal nanomaterials, unexplored avenues that could lead to new fundamental science as well as novel important and useful materials are yet hidden. There is no doubt that this finding will be helpful for further understanding of solution chemistry for the design of different kinds of nanomaterials.

Received: May 9, 2014
Revised: June 23, 2014
Published online: July 30, 2014

Keywords: antimony sulfide · heterostructures · nanocapsules · nanorods · nanotubes

[1] a) O. G. Schmidt, K. Eberl, *Nature* **2001**, *410*, 168; b) R. Tenne, *Angew. Chem.* **2003**, *115*, 5280 – 5289; *Angew. Chem. Int. Ed.* **2003**, *42*, 5124 – 5132; c) K. H. Park, J. Choi, H. J. Kim, J. B. Lee, S. U. Son, *Chem. Mater.* **2007**, *19*, 3861 – 3863; d) L. Ren, M. Wark, *Chem. Mater.* **2005**, *17*, 5928 – 5934; e) M. Brorson, T. W. Hansen, C. J. H. Jacobsen, *J. Am. Chem. Soc.* **2002**, *124*, 11582 – 11583; f) Y. Feldman, E. Wasserman, D. J. Srolovitz, R. Tenne, *Science* **1995**, *267*, 222 – 225; g) C. Ye, G. Meng, Z. Jiang, Y. Wang, G. Wang, L. Zhang, *J. Am. Chem. Soc.* **2002**, *124*, 15180 – 15181.

[2] a) M. Z. Kauser, P. P. Ruden, *Appl. Phys. Lett.* **2006**, *89*, 162104; b) P. Avouris, T. Hertel, R. Martel, T. Schmidt, H. R. Shea, R. E. Walkup, *Appl. Surf. Sci.* **1999**, *141*, 201 – 209; c) A. Modi, N. Koratkar, E. Lass, B. Wei, P. M. Ajayan, *Nature* **2003**, *424*, 171 – 174; d) D. Wang, J. Sun, X. Cao, Y. Zhu, Q. Wang, G. Wang, Y. Han, G. Lu, G. Pang, S. Feng, *J. Mater. Chem. A* **2013**, *1*, 8653 – 8657; e) J. Chen, S.-L. Li, Z.-L. Tao, Y.-T. Shen, C.-X. Cui, *J. Am. Chem. Soc.* **2003**, *125*, 5284 – 5285; f) G. Mpourmpakis, G. E. Froudakis, G. P. Lithoxoos, J. Samios, *Nano Lett.* **2006**, *6*, 1581 – 1583; g) D. T. Mitchell, S. B. Lee, L. Trofin, N. Li, T. K. Nevanen, H. Soederlund, C. R. Martin, *J. Am. Chem. Soc.* **2002**, *124*, 11864 – 11865.

[3] a) X. Peng, U. Manna, W. Yang, J. Wickham, E. Scher, A. Kadavanich, A. P. Allvisatos, *Nature* **2000**, *404*, 59 – 61; b) R. Buonsanti, V. Grillo, E. Carlino, C. Giannini, M. L. Curri, C. Innocenti, C. Sangregorio, K. Achterhold, F. G. Parak, A. Agostiano, P. D. Cozzoli, *J. Am. Chem. Soc.* **2006**, *128*, 16953 – 16970; c) S. Chakrabortty, J. A. Yang, Y. M. Tan, N. Mishra, Y. Chan, *Angew. Chem.* **2010**, *122*, 2950 – 2954; *Angew. Chem. Int. Ed.* **2010**, *49*, 2888 – 2892; d) Y. Shemesh, J. E. MacDonald, G. Menagen, U. Banin, *Angew. Chem.* **2011**, *123*, 1217 – 1221; *Angew. Chem. Int. Ed.* **2011**, *50*, 1185 – 1189; e) J. Park, J. Joo, S. G. Kwon, Y. Jang, T. Hyeon, *Angew. Chem.* **2007**, *119*, 4714 – 4745; *Angew. Chem. Int. Ed.* **2007**, *46*, 4630 – 4660; f) L. Manna, D. J. Milliron, A. Meisel, E. C. Scher, A. P. Alivisatos, *Nat. Mater.* **2003**, *2*, 382 – 385.

[4] a) X. Zheng, Y. Xie, L. Zhu, X. Jiang, Y. Jia, W. Song, Y. Sun, *Inorg. Chem.* **2002**, *41*, 455 – 461; b) R. Tenne, L. Margulis, M. Genut, G. Hodes, *Nature* **1992**, *360*, 444 – 446; c) B. Mayers, Y. Xia, *Adv. Mater.* **2002**, *14*, 279 – 282.

[5] a) R. Bose, G. Manna, N. Pradhan, *Small* **2014**, *10*, 1289 – 1293; b) X. Peng, *Adv. Mater.* **2003**, *15*, 459 – 463; c) M. R. Kim, K. Miszta, M. Povia, R. Brescia, S. Christodoulou, M. Prato, S. Marras, L. Manna, *ACS Nano* **2012**, *6*, 11088 – 11096; d) H.-C. Peng, S. Xie, J. Park, X. Xia, Y. Xia, *J. Am. Chem. Soc.* **2013**, *135*, 3780 – 3783; e) K.-S. Cho, D. V. Talapin, W. Gaschler, C. B. Murray, *J. Am. Chem. Soc.* **2005**, *127*, 7140 – 7147; f) S. Mourdikoudis, L. M. Liz-Marzán, *Chem. Mater.* **2013**, *25*, 1465 – 1476.

[6] a) N. S. Karan, S. Sarkar, D. D. Sarma, P. Kundu, N. Ravishankar, N. Pradhan, *J. Am. Chem. Soc.* **2011**, *133*, 1666 – 1669; b) W. Li, R. Zamani, M. Ibáñez, D. Cadavid, A. Shavel, J. R. Morante, J. Arbiol, A. Cabot, *J. Am. Chem. Soc.* **2013**, *135*, 4664 – 4667; c) R. Bose, G. Manna, N. Pradhan, *J. Phys. Chem. C* **2013**, *117*, 20991 – 20997.

[7] a) H. Jiang, T. Zhao, C. Yan, J. Ma, C. Li, *Nanoscale* **2010**, *2*, 2195 – 2198; b) J. Yang, Y.-C. Liu, H.-M. Lin, C.-C. Chen, *Adv. Mater.* **2004**, *16*, 713 – 716.

[8] J. Gutwirth, T. Wágner, P. Němec, S. O. Kasap, M. Frumar, *J. Non-Cryst. Solids* **2008**, *354*, 497 – 502.

[9] A. K. Guria, S. Sarkar, B. K. Patra, N. Pradhan, *J. Phys. Chem. Lett.* **2014**, *5*, 732 – 736.

[10] a) T. Mokari, E. Rothenberg, I. Popov, R. Costi, U. Banin, *Science* **2004**, *304*, 1787 – 1790; b) X.-H. Li, J. Lian, M. Lin, Y.-T. Chan, *J. Am. Chem. Soc.* **2011**, *133*, 672 – 675.

[11] a) J. Xu, C.-S. Lee, Y.-B. Tang, X. Chen, Z.-H. Chen, W.-J. Zhang, S.-T. Lee, W. Zhang, Z. Yang, *ACS Nano* **2010**, *4*, 1845 – 1850; b) M.-A. Langevin, A. M. Ritcey, C. N. Allen, *ACS Nano* **2014**, *8*, 3476 – 3482.

